

L. KERVEVAN
H. GILLES
S. GIRARD 
M. LAROCHE
P. LEPRINCE

Self-mixing laser Doppler velocimetry with a dual-polarization Yb:Er glass laser

Equipe Lasers, Instrumentation Optique et Applications,
Centre Interdisciplinaire de Recherche Ions Laser (CIRIL), CNRS-CEA-ENSICAEN, UMR 6637,
6 Blvd. Maréchal Juin, 14050 Caen Cedex, France

Received: 9 March 2006/Revised version: 26 July 2006
© Springer-Verlag 2006

ABSTRACT Self-mixing laser Doppler velocimetry using a dual-polarization Yb:Er-doped phosphate glass laser is investigated. The two orthogonally polarized eigenstates emitted simultaneously by the laser oscillator are employed to perform a heterodyne detection, allowing a complete characterization of the lateral sidebands generated via the optical feedback around the beating peak. Two different experimental set-ups have been implemented: (i) direct feedback on one of the two modes or (ii) crosstalk between the two modes via a non-reciprocal Faraday element. The results are analysed and applications to velocity measurements are discussed. Finally, some considerations of the noise correlated in phase and in opposite phase on the two polarization states are also discussed.

PACS 42.55.Xi; 42.60.Rn; 42.81.Pa

1 Introduction

Different non-intrusive optical techniques are commonly used for velocity measurements. Among them, laser Doppler velocimetry (LDV) [1] based on the interference between two coherent optical beams split from a single laser source is certainly the most widely used method in the industry.

Another approach based on the self-mixing effect in class B lasers (a laser with a decay rate by spontaneous emission γ_{sp} significantly lower than the photon decay rate inside the cavity γ_c) has been recently investigated in the literature [2–5]. Basically, the approach is quite similar to LDV as it is also based on the frequency beating between two coherent optical beams. However, in the self-mixing approach, one of the two optical beams (which could be considered as the reference beam) is the optical wave oscillating inside the laser cavity, whereas the second beam is provided via the tiny part of the output beam diffused on the moving target and back reflected inside the cavity mode. Optical sensors based on self-mixing present many advantages over the more sophisticated interferometric optical set-up as being self-aligned, simple to implement and reliable. More-

over, the optical set-up used for velocity measurements could also be easily adapted for applications like vibrometry [6] or optical tomography [7]. But, the main advantage with the self-mixing approach is its intrinsic enhanced sensitivity compared to classical sensors. This could be mainly attributed to the specific dynamics of class B lasers (semiconductor or solid-state lasers), which present some relaxation oscillations under a time-dependant perturbation. When the beating note due to the optical feedback is close to the eigenfrequency of these relaxation oscillations, the laser becomes very sensitive to any small coherent feedback. The result is a significant enhancement in the amplitude response on low cooperative targets as the laser oscillator plays simultaneously two roles: (i) a coherent light source and (ii) an optical interferometer that mixed and amplified the beating note due to the Doppler shift [5]. This internal amplification allows a signal-to-noise ratio only limited by the laser quantum noise (noise related to the spontaneous emission in the amplifying medium).

Among the different evolutions that could be applied to the basic principles of LDV or self-mixing, determination of the velocity sign is an important issue (for example to observe flow reversal in complicated flow patterns). In the LDV set-up, it is obtained thanks to an external optical frequency shifter located on one of the two optical laser beams. The shifter allows heterodyne detection around the beating frequency.

In the case of self-mixing experiments with class B solid-state lasers, the frequency shift must be adjusted close to the relaxation oscillation frequency to enhance the response of the laser to the optical feedback. A technique using a pair of acoustic Bragg cells [8] driven at slightly different frequencies has already been investigated. However, it is quite complicated to align and not very easy to handle for practical applications.

For self-mixing, it could therefore be interesting to develop a completely passive method based on the intrinsic properties of the laser source to obtain the velocity sign. In the case of laser diodes, the detected signals present a sawtooth-like structure when the optical feedback is at a moderate injection level (known as the $C > 1$ condition) [9]. The form of the sawtooth signal suppresses the sign ambiguity in both velocity and displacement measurements [9, 10]. However, this method is not usable through very weak optical feedback as the beating signal tends to become purely sinusoidal.

 Fax: +33-2-31-45-25-57, E-mail: sylvain.girard@ensicaen.fr

Another approach consists of using a quasi-isotropic laser with two orthogonally polarized eigenstates that simultaneously oscillate into the cavity with slightly different frequencies. This technique has already been reported using a dual-polarization Zeeman He-Ne laser [11] but such a laser presents only limited sensitivity to optical feedback. The possibility of using a dual-polarization class B solid-state laser for velocity measurement has also been briefly reported by Nerin et al. [12] but with only limited discussion about the physical advantages of using such a laser.

In the present paper, a dual-polarization Yb:Er-doped phosphate glass laser was built to further explore the combination between optical feedback and passive heterodyne detection using a quasi-isotropic laser with two eigenstates. The first part of the paper describes the laser cavity and the experimental set-up. By adjusting the relative angular orientation of two quarter-wave plates inserted inside the cavity, it becomes possible to adjust the beating frequency close to the relaxation oscillation frequency, exalting the specific dynamics of this class B laser. Two configurations for this passive self-heterodyne detection via the dual-polarization eigenstate laser were investigated for velocimetry measurements. The second part of the paper contains a simple theoretical modelling for the two approaches. A comparison between the models and the experimental results obtained is provided. Finally, some further applications of the concept are suggested as well as possible intrinsic noise reduction to improve the signal-to-noise ratio.

2 Experimental set-up

The two experimental set-ups used during the present investigation are illustrated in Fig. 1a and b. They are basically similar except considering the optical feedback applied to the laser. In both cases, the experiment is based on a quasi-isotropic diode-pumped solid-state laser submitted to a polarization-controlled optical feedback. The amplifying medium was a 710- μm -thick phosphate glass disc co-doped with 0.8% Er^{3+} and 20% Yb^{3+} . This amorphous laser material has been preferred to more classical Nd-doped crystalline amplifying media already used for self-mixing on solid-state lasers ($\text{Y}_3\text{Al}_5\text{O}_{12}$ or $\text{LiNdP}_4\text{O}_{12}$) as it presents many interesting and favourable properties for self-mixing. First of all, as already stated elsewhere [4, 13], the long spontaneous emission lifetime of the $^4I_{13/2}$ level for Er^{3+} ions in phosphate glass ($\tau_{\text{sp}} = 8$ ms) is favourable to enhance the sensitivity of the laser to a weak optical feedback. Moreover, Er^{3+} -doped phosphate glass lasers emit near 1535 nm, into the so-called eye-safe spectral domain. It allows using the laser beam in a free atmospheric propagating mode with significantly limited specific care considering the laser safety. Moreover, as this spectral domain also corresponds to the telecom optical fibre market, it becomes possible to instrument the laser using standard optical components (fibre, modulator and so on). Finally, the Er:Yb glass medium is an isotropic material which is an imperative condition to obtain simultaneously two orthogonally polarized eigenstates [14, 15]. The cavity should contain no dichroic element (especially not the amplifying medium) to keep a similar laser threshold for the two orthogonally polarized modes. Therefore, the stimulated emission

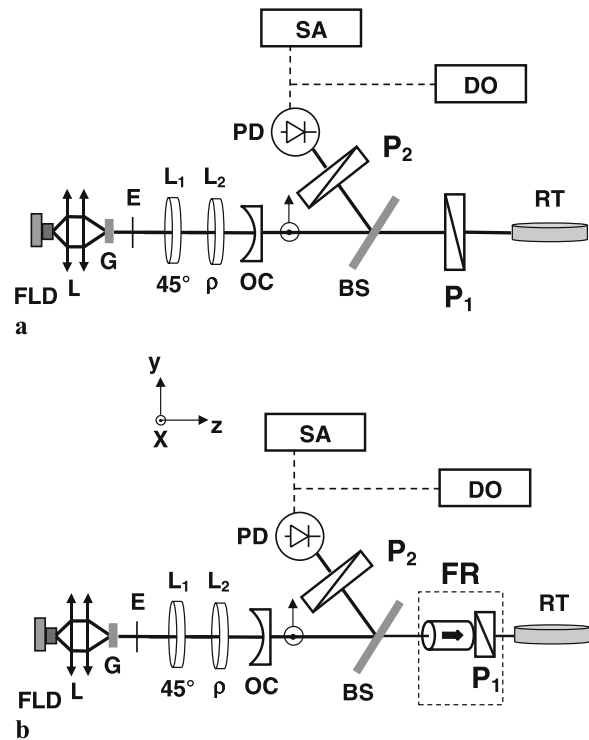


FIGURE 1 Experimental set-up: DO, digital oscilloscope; SA, rf spectrum analyser; FLD, fiber laser diode; G, Yb:Er glass; E, etalon; OC, output coupler; L, lens; L_1 , L_2 , quarter-wave plates ($\lambda/4$); BS, beam splitter; PD, InGaAs photodiode; FR, Faraday rotator; RT, rotating target

cross sections should be exactly the same, independently of the electric field polarization state inside the cavity.

The laser oscillator is formed by a simple hemispherical cavity. The active medium plate is located near the waist of the cavity. One of its faces is directly coated to form the planar dielectric input mirror ($R = 99, 98\%$ at 1535 nm and $T > 90\%$ at 980 nm), whereas the other face is antireflection coated near 1535 nm. The cavity length is adjusted to $L = 90\text{--}100$ mm with a concave output coupler (radius of curvature $\text{ROC} = 100$ mm; the intensity transmission coefficient is given by $T = 2\%$ near 1535 nm). The active medium is longitudinally pumped at 980 nm using a 1.5-W fibre-pigtailed laser diode (Roithner, reference G098PU11500M). The optical fibre is multimode with a core diameter of 100 μm . A fibre-coupled laser diode was preferred compared to a bulk semiconductor laser as the optical fibre ensures a perfectly circular transverse gain mode inside the amplifying medium. It favours an isotropic behaviour of the laser cavity and significantly simplified the oscillation simultaneously on dual-polarization orthogonal states. A silica etalon E (thickness $e = 200$ μm , coated on both faces with a reflection coefficient $R = 30\%$ at 1.53 μm) was inserted for longitudinal mode selection.

The beating frequency between the two modes can be experimentally detected on a photodiode (PD) by adding a linear polarizer oriented at 45° versus the two polarization eigenstates (polarizer P_2 in Fig. 1). The beating note depends on the characteristics of the pumping beam (optical power and spatial distribution inside the active medium) and varies from a few MHz up to a few dozens of MHz. It can be precisely adjusted by controlling the pump power and the alignment and/or length of the resonator. In order to precisely tune the

beating frequency, two quarter-wave plates (L_1 and L_2) were introduced inside the cavity. The neutral optical axes of L_1 were oriented at 45° compared to the two polarization eigenstates that already oscillate naturally inside the cavity. The slow axis of L_2 was then oriented at an angle Q with respect to the fast axis of L_1 . If we neglect the birefringence induced inside the amplifying medium, the beating frequency imposed by the two quarter-wave plates can be calculated using Jones matrix formalism as being [16]

$$\Delta\nu_{\text{Beat}} = \nu_y - \nu_x = \frac{\omega_y - \omega_x}{2\pi} = \frac{QC}{\pi L}, \quad (1)$$

where c is the speed of light, $\nu_{x(y)}$ are the frequencies corresponding respectively to the two orthogonally polarized eigenstates oriented along the x (y) axis and L is the cavity length.

The optical set-up with the two quarter-wave plates allows controlling carefully the beating frequency and adjusting it close to the relaxation oscillation frequency or far away from the relaxation frequency. In the case of the present Yb:Er-doped phosphate glass laser, the relaxation oscillation frequency is close to 80 kHz. Moreover, as the two modes can be optically coupled via the optical feedback, it allows adjusting the frequency difference close to the relaxation frequency to fully benefit from the exaltation of the laser dynamics in a self-mixing experiment.

The two configurations used during the present investigation are represented in Fig. 1a and b, respectively. As already briefly mentioned, these two configurations only differ by the optical feedback applied on the laser cavity. In both cases, a small part of the incident beam is picked up thanks to a beam splitter and photodetected on an InGaAs photodiode (Thorlabs, model PDA 400). The signal can be simultaneously analysed temporally using a digital oscilloscope (Lecroy, model Wavesurfer 432) or spectrally thanks to a radio-frequency (rf) spectrum analyser (Agilent, model E4402B). During the experiments, the dual-polarization solid-state laser was mainly investigated for velocity measurements. Therefore, the laser beam was sent to a moving target which consisted of the edge of a rotating disc. It allows creating an adjustable Doppler shift on the optical feedback which is denoted $\Delta\nu_{\text{Doppler}}$. The angle value between the laser beam and the speed vector of the rotating disc is adjusted around 45° during the experiments. The small part of the diffused light beam coherently backscattered inside the laser cavity mode perturbs its behaviour via a self-mixing effect. The amount of back-reflected light inside the oscillating mode could be estimated from previous experiments at 10^{-8} – 10^{-10} times the incident power.

In the case of Fig. 1a, a linear polarizer called P_1 selects one of the two polarized eigenstates. This mode corresponds to an optical frequency denoted ν_x and is the mode directly affected by the optical feedback. The re-injected light is frequency shifted at $\nu_x + \Delta\nu_{\text{Doppler}}$. The second mode, at a slightly different optical frequency ν_y , remains unchanged and only serves as a reference oscillator for the heterodyne detection. The frequency mixing between the optical signal at $\nu_x + \Delta\nu_{\text{Doppler}}$ and the reference at ν_y is provided by a second polarizer P_2 located in front of the photodiode and oriented at 45° for mixing between the two modes.

In the case of the configuration illustrated in Fig. 1b, a Faraday rotator inserted in the optical path between the out-

put coupler and the target allows coupling the two polarization states via the optical feedback. The angular orientation of the Faraday rotator is adjusted in order to rotate each of the two orthogonally polarized modes by 45° for each pass. The polarizer P_1 selects only one of the two modes, for example the one corresponding to the frequency ν_x . The non-reciprocal nature of the Faraday magneto-optical effect ensures that the eigenstate corresponding to the frequency ν_x will be optically coupled via the optical feedback to the second mode at frequency ν_y . When the optical feedback is frequency shifted by the rotation of the disc, its frequency becomes $\nu_x + \Delta\nu_{\text{Doppler}}$. When it is mixed into the cavity with the mode corresponding to the frequency ν_y , it creates a frequency beating note at the frequency $\nu_x + \Delta\nu_{\text{Doppler}} - \nu_y$ directly obtained on the photodiode without the help of the polarizer P_2 .

3 Theoretical model of self-mixing on dual-frequency laser

Dynamics and intensity noise of class B solid-state lasers emitting simultaneously on two longitudinal modes have already been extensively studied [17]. The rate equations must be divided into two classes respectively associated with the two modes that simultaneously oscillate inside the cavity. Let us denote the population inversions n_x and n_y and the intensities I_x and I_y associated respectively with the two polarization eigenstates oriented along the axes x and y , respectively. Following similar notation already used in [15], the rate equations can be written

$$\begin{cases} \frac{dn_{x(y)}(t)}{dt} = \Gamma_p - \gamma_{\text{sp}}n_{x(y)}(t) \\ \quad - (\beta_{x(y)}I_{x(y)} + \theta_{xy(yx)}I_{x(y)})n_{x(y)}, \\ \frac{dI_{x(y)}(t)}{dt} = -\gamma_c I_{x(y)} + \kappa n_{x(y)}I_{x(y)}, \end{cases} \quad (2)$$

with Γ_p the pumping rate on each of the two orthogonal modes, γ_{sp} the spontaneous decay rate of the emitting level and $\beta_{x(y)}$ and $\theta_{xy(yx)}$ the self- and cross-saturation coefficients. In a two-mode class B laser, the intensity noise is dominated by two relaxation oscillations. One relaxation oscillation peak – corresponding to the highest frequency ν_R – is in phase on the two modes and corresponds to the classical relaxation oscillation peak already reported earlier by McCumber [18] for a single-mode class B laser. Using the rate equations, it could be attributed to the self-saturation term. The second relaxation peak at lower frequency ν_L is attributed to the cross-saturation term between the two modes. For a solid-state laser, the cross saturation is due to the nonlinear coupling because of the spatial overlap between the two modes inside the amplifying medium. On the detected intensities, it appears in opposite phase on the two modes. This second relaxation oscillation peak can only be observed experimentally by detecting each individual mode I_x (or I_y) using a polarization cube beam splitter, but it completely vanished on the total output intensity $I_x + I_y$. Similar observations have already been reported on a dual-polarization microchip Yb:Er glass laser [15]. Introducing Lamb's coupling constant C defined as [17]

$$C = \frac{\theta_{xy}\theta_{yx}}{\beta_x\beta_y}, \quad (3)$$

it becomes straightforward to show that C could be related to the relaxation oscillation frequencies using

$$C = \left(\frac{1 - (\nu_L/\nu_R)^2}{1 + (\nu_L/\nu_R)^2} \right)^2. \quad (4)$$

In the present series of experiments, the two orthogonally polarized modes have optical frequencies only slightly separated and are adjusted to obtain equal average intensities $\langle I_x \rangle = \langle I_y \rangle$ in the stationary regime. Therefore, it could be assumed that $\beta_x = \beta_y$ and $\theta_{xy} = \theta_{yx}$. Moreover, the strong overlap between the standing waves in the amplifying medium leads to a strong coupling between the modes. Observing the relaxation oscillation peaks, we have measured typically $\nu_L = 10\text{--}20$ kHz, whereas $\nu_R = 80\text{--}100$ kHz depending on the cavity alignment and beating note frequency between the two modes. The coupling constant C is above 0.9 and could be considered close to unity. Therefore, it is assumed that $\beta_x = \beta_y = \theta_{xy} = \theta_{yx} = \beta$.

Following the initial approach developed by Lang and Kobayashi [19] for a semiconductor laser and re-adapted by Lacot et al. [20] for a four-level solid-state system, the optical feedback can be correctly described for a three-level solid-state laser using the rate equations of a re-injected laser. In the case of a dual-polarization laser, the dynamics is fully described using four coupled rate equations: two equations describing the evolution of the population inversion associated with modes x and y (as in (2)) and two equations for the two orthogonally polarized electric fields E_x and E_y oscillating simultaneously inside the resonant cavity. Amplitudes E_x and E_y (instead of the associated intensities I_x and I_y used in (2)) are necessary in the case of optical feedback as re-injection creates some phase-dependent interference effects inside the cavity. The rate equations correspond to

$$\begin{cases} \frac{dn_{x(y)}(t)}{dt} = (W_p - \gamma_{sp}) \frac{n_T}{2} - (W_p + \gamma_{sp}) n_{x(y)}(t) \\ \quad - 2B(I_x(t) + I_y(t)) n_{x(y)}(t), \\ \frac{dE_{x(y)}(t)}{dt} = \left(i\omega_{x(y)} + \frac{1}{2}(Bn_{x(y)}(t) - \gamma_c) \right) E_{x(y)}(t) \\ \quad + \gamma_{\text{ext}} E_{\text{inj},x(y)}(t), \end{cases} \quad (5)$$

where n_T is the total population density, $\omega_{x(y)} = 2\pi\nu_{x(y)}$ are the free-running laser frequencies for each mode without optical feedback, W_p is the pumping rate per ion in the fundamental level, γ_c is the photon decay rate in the cavity, γ_{sp} is the spontaneous decay rate of the ${}^4I_{13/2}$ emitting level and B is the Einstein coefficient. All the external factors like projection of the back-diffused field on the transverse mode of the laser, transmission of the output coupler (emission and reception) and contribution of the target are taken into account in the factor γ_{ext} . In (5), the total intensity $I(t) = I_x(t) + I_y(t)$ could be expressed versus the electric field amplitude of the two orthogonally polarized modes as

$$I_x(t) + I_y(t) = |\mathbf{E}_x + \mathbf{E}_y|^2. \quad (6)$$

Here $E_{x(y)}$ are the electric fields for the two polarization eigenstates and could be defined as follows:

$$\mathbf{E}_{x(y)} = E_{cx(y)}(t) e^{j(\omega_{x(y)}t + \varphi_{x(y)}(t))} \mathbf{u}_{x(y)}, \quad (7)$$

where $\mathbf{u}_x \perp \mathbf{u}_y$ are the unit vectors associated with the two polarization states. The electric field due to the optical feedback is labelled $E_{\text{inj},x(y)}$. The amplitude can be related to E_x or E_y depending on the polarization selection operated outside the cavity, whereas the phase of this complex field is calculated just before the re-injection through the output coupler. The total round-trip time of flight between the laser and the target is defined as τ and is linearly proportional to the distance D between the laser and the target ($\tau = 2D/c$). Depending on the geometry used for the experiment, two distinctive expressions for $E_{\text{inj},x(y)}(t)$ can be formulated.

In the case of Fig. 1a, $E_{\text{inj},x}(t)$ and $E_{\text{inj},y}(t)$ become

$$\begin{cases} E_{\text{inj},x}(t) = E_{cx}(t - \tau) e^{j((\omega_x + \Omega_D)(t - \tau) + \varphi_x(t - \tau))} \mathbf{u}_x, \\ E_{\text{inj},y}(t) = \mathbf{0}, \end{cases} \quad (8)$$

where $\Omega_D = 2\pi \Delta \nu_{\text{Doppler}}$ represents the frequency shift due to the Doppler effect on a moving target.

In the case of Fig. 1b, $E_{\text{inj},x}(t)$ and $E_{\text{inj},y}(t)$ become

$$\begin{cases} E_{\text{inj},x}(t) = \mathbf{0}, \\ E_{\text{inj},y}(t) = E_{cy}(t - \tau) e^{j((\omega_y + \Omega_D)(t - \tau) + \varphi_y(t - \tau))} \mathbf{u}_y. \end{cases} \quad (9)$$

In this second geometry, the electric field E_x is selected at the emission and re-injected on the mode corresponding to the electric field E_y via the non-reciprocal Faraday element.

Without any optical feedback ($\gamma_{\text{ext}} = 0$) and assuming that $\omega_{x(y)} \approx \omega_c$ (that is to say neglecting the break of degeneracy between the two modes) and similar intensities for the two modes $I_x = I_y = I_{\text{tot}}/2$ ($E_x = E_y = E/\sqrt{2}$) (that is to say neglecting all the noise effect), it becomes straightforward to deduce a stationary solution for the set of equations (5). It corresponds to the classical steady-state solutions for a three-level laser system:

$$\begin{cases} n(t) = n_x + n_y = n_s = \frac{2\gamma_c}{B}, \\ I(t) = E^2(t) = E_s^2 = E_{\text{sat}}^2 \left(\frac{\beta}{\beta_s} - 1 \right), \end{cases} \quad (10)$$

where $\beta = (W_p - \gamma_{sp})/(W_p + \gamma_{sp})$, $\beta_s = n_s/n_T$ and $E_{\text{sat}}^2 = (W_p + \gamma_{sp})/2B$. Here $E(t)$ is a fictitious scalar electric field used to describe the total intensity for the two modes $I(t) = E^2(t) = I_x + I_y$. For a laser submitted to a low amount of optical feedback ($\gamma_{\text{ext}} \ll \gamma_c$), it is easy to solve analytically the set of differential equations (5) assuming that the optical feedback induces a small perturbation compared to the electric field in the steady-state regime. In this case, first-order perturbation can be assumed and the population inversion and the electric fields are only slightly modified as

$$\begin{cases} n(t) = n_s + \Delta n(t), \\ E_{cx}(t) = E_{sx} + \Delta E_{cx}(t), \\ E_{cy}(t) = E_{sy} + \Delta E_{cy}(t), \end{cases} \quad (11)$$

where $E_{sx} = E_{sy} = E_s/\sqrt{2}$.

From (5), (7), (10) and (11), a set of differential equations for $\Delta n(t)$ and $\Delta E_{cx(y)}(t)$ can be easily established in the two cases corresponding respectively to (8) or (9). The resulting perturbation on the electric field can be used to calculate the

intensity detected on the quadratic detector (photodiode PD) located after the polarizer P_2 . Here it is assumed that the polarizer P_2 is oriented at 45° compared to the polarization eigenstates which ensure the optical mixing between the two modes. The laser intensity detected on the photodiode can be expressed as

$$I_{\text{ph}} = \frac{I_s}{2} \left[1 + \cos((\omega_x - \omega_y)t + \Delta\varphi) + \gamma_{\text{ext}}\gamma_E(\omega_{\text{feedback}}) \cos(\Omega_D t + \Delta\varphi') + \gamma_{\text{ext}}\gamma_E(\omega_{\text{feedback}}) \cos((\omega_x - \omega_y + \Omega_D)t + \Delta\varphi'') \right], \quad (12)$$

with $\omega_{\text{feedback}} = \Omega_D$ in the case of Fig. 1a and $\omega_{\text{feedback}} = \omega_x - \omega_y + \Omega_D$ for the geometry of Fig. 1b. The factor $\gamma_E(\omega)$ depends on the different parameters appearing in (5) as well as on the relaxation oscillation pulsation Ω_R . They are defined as

$$\left\{ \begin{array}{l} \gamma_E(\omega) = \frac{\sqrt{(W_p + \gamma_{\text{sp}})^2 \left(\frac{\beta}{\beta_s}\right)^2 + \omega^2}}{\sqrt{(\omega^2 - \Omega_R^x)^2 + (W_p + \gamma_{\text{sp}})^2 \left(\frac{\beta}{\beta_s}\right)^2}} \omega^2, \\ \Omega_R^x = \frac{1}{\sqrt{2}} \sqrt{(W_p + \gamma_{\text{sp}})\gamma_c \left(\frac{\beta}{\beta_s} - 1\right)}, \end{array} \right. \quad (13)$$

where $\Omega_R^x = 2\pi\nu_R^x$ represents the relaxation oscillation frequency specific for the polarization state x perturbed via the optical feedback. It is peculiar to a dual-polarization laser and could be related to the classical relaxation oscillation frequency $\Omega_R = 2\pi\nu_R$ affecting the total intensity noise of a three-level solid-state class B laser by $\Omega_R^x = \Omega_R/\sqrt{2}$. The factor $1/\sqrt{2}$ is similar to the relationship between the eigenfrequency of two coupled mechanical or electrical oscillators and the eigenfrequency of one of the two oscillators when the second is looked.

In (12), we can separate three contributions. The first contribution is a beating note due to the optical mixing on polarizer P_2 between the two modes without the optical feedback ($\gamma_{\text{ext}} = 0$). The second modulated term corresponds to the beating note between the oscillating mode and the optical feedback with a mixing inside the cavity. Finally, the third term is a beating note between the perturbed and unperturbed modes with a mixing on the polarizer P_2 .

In the theoretical model, one can wonder why no resonance on the optical feedback sensitivity of the laser appears near the second low frequency relaxation oscillation peak at $\Omega_L = 2\pi\nu_L$. In fact, the term is missing in the model because of the hypothesis that $C = 1$, which leads to $\Omega_L = 0$. Therefore, the simplifying hypothesis makes the second peak completely vanishing in the model. A more complete development without the simplifying hypothesis could conduct to a more complex term $\gamma_E(\omega)$ in (13).

4 Experimental results

Before discussing the potential of such a dual-frequency laser for self-mixing detection, the optical properties of the Yb:Er:glass laser were briefly studied. The first

characterization of the laser output has been obtained without any birefringent plates inserted inside the cavity. In this case, the laser already oscillates on two partially coupled orthogonally polarized modes with two slightly different frequencies. The frequency difference between the two modes is attributed to the thermal stress pump induced into the active medium. It creates a small optical anisotropy inside the amplifying medium, which allows splitting of the oscillating mode into two orthogonally polarized optical modes with slightly different frequencies. However, only a limited control of the beating note frequency is allowed using thermal stress [15].

To adjust precisely the beating frequency, two quarter-wave plates were inserted inside the cavity with an angle ϱ between the neutral axes of the two quarter-wave plates controlled mechanically using a rotating mount. The detection is ensured after the polarizer P_2 . The beating signal only appears when the polarizer is rotated at 45° compared to the two polarization modes, whereas it completely vanishes when the polarizer selects only a single mode.

The beating note frequency between the two orthogonal modes was measured versus the angular tilt. Figure 2a shows the beating signal frequency continuously tunable versus the

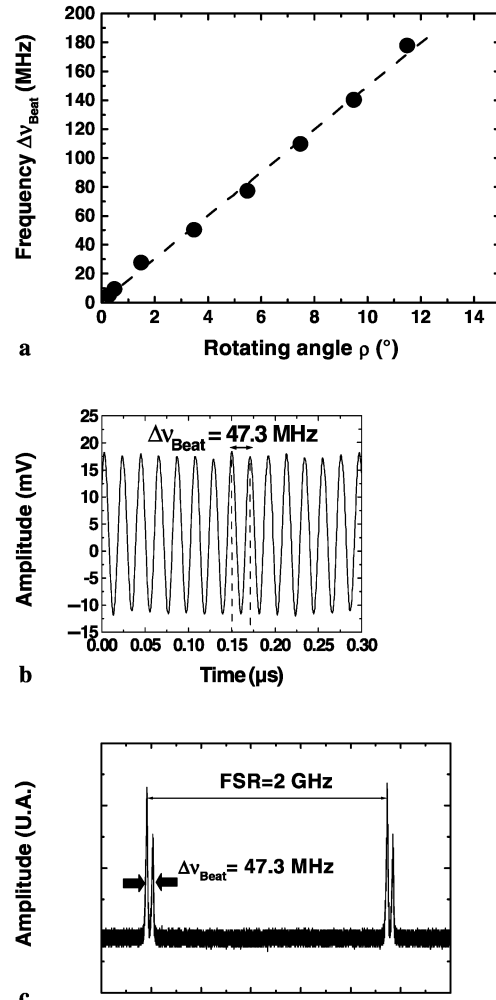


FIGURE 2 Characterization of laser in dual frequency regime: (a) evolution of beating frequency $\Delta\nu_{\text{Beat}}$ versus the rotating angle of the second quarter-wave plate ϱ ; (b) temporal signal; (c) optical spectrum

angular rotation of the quarter-wave plate L_2 . Figure 2b shows the detected signal versus time for $\varrho = 3.6^\circ$, whereas Fig. 2c represents the corresponding optical spectrum obtained from a Fabry-Pérot optical spectrum analyser (Burleigh, model RC-46; free spectral range equal to 2 GHz, finesse allowing a spectral resolution of 10 MHz). A good agreement is obtained between the temporal beating signal and the optical frequency difference between the two orthogonal modes.

A first series of experiments on self-mixing with a dual-polarization laser was based on the experimental set-up schematically drawn in Fig. 1a. The beating note between the two polarization states is adjusted between 500 kHz and a few MHz by adjusting the angle ϱ close to zero. Using polarizer P_1 , a single polarization mode is perturbed via the optical feedback. For the sake of clarity, it can be assumed that the polarizer P_1 selects the polarization state oriented along the x axis. As already stated in the theoretical part of the paper, this case corresponds to a classical heterodyne detection. Here the heterodyne mixing between the two orthogonally polarized modes is obtained outside the cavity using the polarizer P_2 . The non-perturbed polarization state only serves as a reference. The rf spectra observed using this geometry are reported in Fig. 3a and b for a Doppler frequency shift equal to $\Delta\nu_{\text{Doppler}} = 365$ kHz. During the velocity measurements, the optical beam is simply collimated and not focused on the target to limit the effect attributed to the speckle. Compared to the classical approach with direct optical feedback on a single-mode solid-state laser [4, 5], two peaks containing the information on the target velocity appear in the rf spectrum. The first peak is observed at frequency $\Delta\nu_{\text{Doppler}}$. It corre-

sponds to the beating note usually observed on a single-mode laser. Its frequency only depends on the absolute velocity of the target but not on its direction. It appears unchanged when the rotating sense of the disc is reversed, as shown in Fig. 3b. Compared to the theoretical model, it corresponds to the second term appearing in (12). This term appears experimentally when the polarizer P_2 is oriented at 45° or parallel to the axis x (polarizer P_1), whereas it disappears when detecting the polarization mode y .

The second beating peak that contains information on target velocity is located at a frequency $\nu_m = \nu_x - \nu_y + \Delta\nu_{\text{Doppler}} = \Delta\nu_{\text{Beat}} + \Delta\nu_{\text{Doppler}}$. It corresponds to the heterodyne detection via the optical mixing between the two modes on the polarizer P_2 . Compared to the beating note between the two polarization states (adjusted near $\Delta\nu_{\text{Beat}} = 830$ kHz in Fig. 3), the peak due to the Doppler-shifted optical feedback appears as a single-sideband modulation. Depending on the sense of the disc spin, it appears below or above the beating note, as illustrated by comparing Fig. 3a and b. Its relative position compared to the beating note allows determining simultaneously the speed and the rotation sense of the disc. As expected, its amplitude is almost similar to the amplitude of the beating signal due to the homodyne detection. Therefore, it presents a resonant enhancement close to the relaxation oscillation frequency $\Omega_R = 2\pi\nu_R$ as expected theoretically (see (12)). In Fig. 3, the beating note was adjusted at a relatively low frequency (830 kHz) to record simultaneously all the terms of (12) on the same rf spectrum. Of course, it is also possible to adjust the beating note at higher frequency (a few hundred MHz, for example) while keeping the signal containing the Doppler shift close to the beating note with similar amplitude. This configuration allows filtering and amplifying selectively the detected signal around the beating frequency, as in a classical heterodyne detection. Of course, the measurement range is intrinsically limited by the dynamics of the class B laser. Considering (13) for the factor $\gamma_E(\omega)$, the laser acts as a pass-band filter around the beating signal with signal-to-noise ratio kept above 30 dB for a Doppler shift between 0 and a few MHz.

The relaxation oscillation corresponds to a peak noise at 80 kHz on the rf spectra reported in Fig. 3a and b. As expected, the relaxation oscillation noise at high frequency ($\Omega_R = 2\pi\nu_R$) appears in phase on the two orthogonal modes and is of course reported on the beating signal when the two modes are mixed via the polarizer P_2 . Typically, the optical feedback bandwidth of the laser submitted to a Doppler shift can be considered around a few dozen times the relaxation oscillation frequency. As for the beating note, the signal corresponding to the heterodyne detection (third term in (12)) almost completely vanished when the polarizer P_2 only selects one of the two polarization modes.

The second series of experiments on self-mixing with a dual-polarization laser was done using a Faraday element to couple the two polarization modes via the optical feedback, as illustrated in Fig. 1b. Therefore, it becomes possible to couple selectively the mode x on the mode y via the optical feedback while keeping the mode x unperturbed by the mode y . As expected theoretically from (12) and (13), the results are almost exactly similar to the result obtained before as soon as the beating note is kept close to the relaxation oscillation

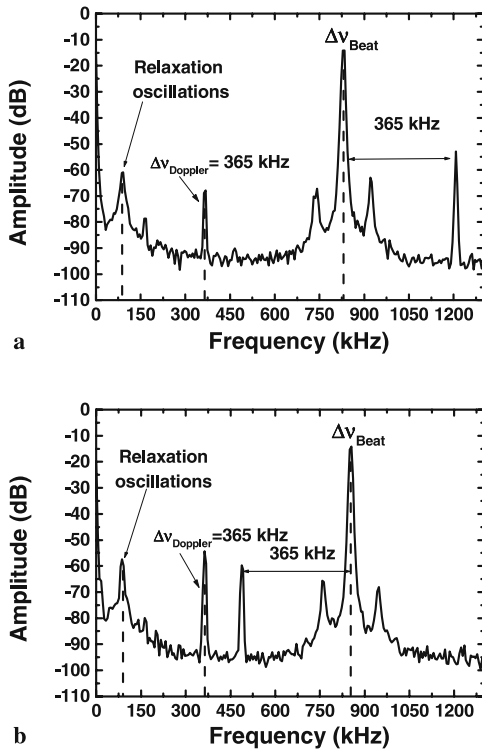


FIGURE 3 Radio-frequency spectra of the detected signal in heterodyne detection with a simple linear polarizer (set-up (a) of Fig. 1): (a) disc turning clockwise; (b) disc turning anticlockwise

frequency. For example, the two spectra recorded comparatively without the Faraday rotator (but still with the polarizer P_1) and with the Faraday element P_1 are shown in Fig. 4a and b for a Doppler shift equal to 298 kHz. Apparently, no clear difference appears between the two configurations. However, by adjusting the orientation of the polarizer P_2 , it becomes possible to show that the Faraday element allows coupling of the two polarization modes via the optical feedback. For example, when the polarizer P_2 is re-oriented perpendicular to the polarization state selected using the polarizer P_1 , the same peak attributed to the beating between the two modes via the optical feedback still appears in the rf spectrum. It shows that the beating mode observed is now mainly due to the optical frequency mixing inside the laser cavity rather than on the polarizer P_2 . On the other hand, when the polarizer P_2 selects the mode unaffected by the optical feedback, no beating mode appears in the rf spectrum.

The main difference between the heterodyne detection (illustrated in Fig. 1a) and the optical mixing between the two modes via the optical feedback (Fig. 1b) is that the second approach allows extending artificially the dynamical range of velocity measurement for the self-mixing technique in a class B solid-state laser. The fine tuning of the frequency difference between the two modes gives the possibility to adjust the beating note to compensate almost completely the Doppler frequency shift on the moving target. In this case, the frequency beating $\Delta\nu_{\text{Beat}}$ between the two modes is still clearly observable in the rf spectra using polarizer P_2 , while the difference between this peak and the beating note $\nu_m = \Delta\nu_{\text{Beat}} + \Delta\nu_{\text{Doppler}}$ corresponds exactly to the Doppler shift. If the frequency difference between the two polarization eigenstates is adjusted to keep the beating note close to the relaxation oscillation frequency, the self-mixing technique will present a good sensitivity, even for a very small amount of optical feedback. Therefore, the adjustment of $\Delta\nu_{\text{Beat}}$ over half of the free spectral range of the laser cavity (as allowed following (1)) leads to a significant extension of the dynamical range of measurement of $\Delta\nu_{\text{Doppler}}$ using the dual-frequency laser system. To illustrate this last point, the two quarter-wave plates were re-oriented at $\varrho = 1.2^\circ$ to obtain a frequency beating around 10 MHz. When the disc rotation speed increases, the Doppler shift can be adjusted up to a few MHz. In this case, the peak due to the optical coupling between the two modes via the Faraday rotator appears at significantly low frequency and close to the relaxation oscillation frequency peak. As illustrated in Fig. 5, the peak due to the non-reciprocal coupling between the two modes becomes higher than the peak due to the traditional self-mixing term. Its clearly illustrates the intrinsic advantages of a dual-polarization laser to offer a possible extension of the measurement range via self-mixing.

Finally, one can wonder if the dual-frequency laser would also permit us to improve the signal-to-noise ratio using one of the two modes as a reference for the intensity noise. It has been checked experimentally that the relaxation oscillation peaks at higher frequency appear in phase on the two modes. In this case, detection simultaneously on the two modes would allow reducing the noise affecting the polarization modes used for the measurement by deducing the noise affecting the second polarization mode. Some experiments were done but no clear

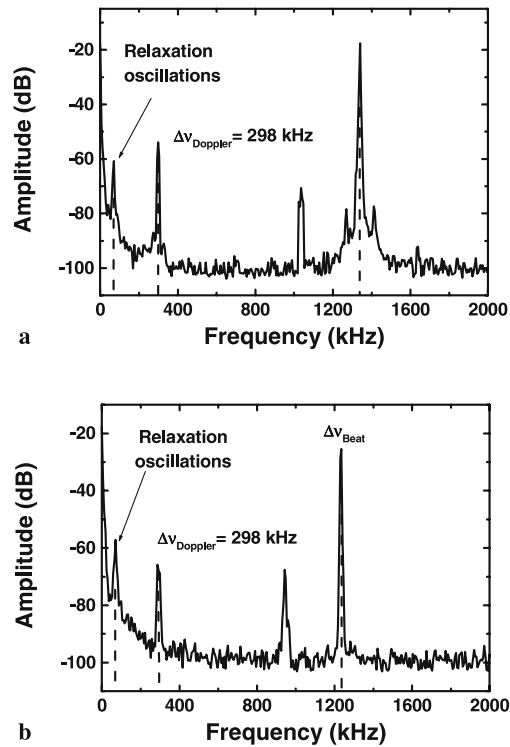


FIGURE 4 Comparison between the rf spectra of the detected signal without Faraday rotator (a) and with Faraday rotator (b)

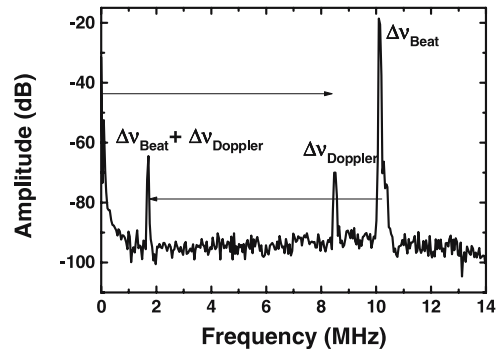


FIGURE 5 Radio-frequency spectrum with a Faraday rotator and a large beating note between the two modes to show the extension of the velocity range measurement

evidence at the moment appears on the real advantage of such a technique as the correlation between intensity noises on the two modes appears only near the relaxation oscillation peaks.

5 Conclusion

Dual-frequency solid-state lasers have been proved as very promising tools for different practical applications based on heterodyne detection (such as lidar [21], rf-to-optical conversion and so on). The present paper deals with the opportunity to use a solid-state dual-frequency laser for self-mixing detection. In this technique, the laser plays simultaneously different roles: a coherent optical source, an interferometer and an amplifier. Self-mixing using solid-state lasers has long been recognized as yielding very sensitive, self-aligned and reliable optical sensors. However, the heterodyne detection for optical feedback is usually based on the use of an

external frequency shifter with an acousto-optic modulator. Here the frequency shifting is directly provided via the beating note between the two modes on a dual-polarization-state diode-pumped Yb:Er:glass laser. After a brief presentation of the laser properties, two different configurations for the optical feedback have been investigated. The first configuration consists of using the heterodyne detection to determine the sense of the velocity without using a further optical frequency shifter. The optical feedback is done selectively on one of the two polarization states, whereas the detection is done near the beating note via optical mixing with the second mode. This original approach gives access to the sense. Moreover, the second approach in which the optical feedback mixed the two modes via a Faraday element has also been investigated. This approach allows extending significantly the velocity range available from the self-mixing technique in solid-state class B lasers.

Further improvements would need a better and simpler control of the optical frequency difference between the two modes. For example, it is possible to use an electro-optic phase shifter integrated directly inside the cavity instead of the two wave plates. This technical improvement would significantly simplify the tuning method between the two modes, as it could be controlled with a simple voltage signal. It should give a real extension to the possible adjustment of the velocity range in the case of optical coupling between the two modes via the non-reciprocal effect. Moreover, investigations of the response of the laser near the low frequency relaxation oscillation peak could also become interesting as they would allow us to extend the dynamics at very low velocity (observation of Brownian particle movement, for example [22]). However, such investigations would need to review the theoretical models, as they should be developed with fewer sim-

plifications to keep the relaxation oscillation peak at a low frequency.

ACKNOWLEDGEMENTS This research was supported by Pole ITIC (Image et Technologie de l'Information et de la Communication) under contract 2000-2006.

REFERENCES

- 1 F. Durst, A. Melling, J.H. Whitelaw, *Principles and Practice of Laser-Doppler Anemometry* (Academic, New York, 1976)
- 2 T. Bosch, N. Servagent, S. Donati, *Opt. Eng.* **40**, 20 (2001)
- 3 P.A. Porta, D.P. Curtin, J.G. McInerney, *IEEE Photon. Technol. Lett.* **14**, 1719 (2002)
- 4 L. Keruevan, H. Gilles, S. Girard, M. Laroche, *IEEE Photon. Technol. Lett.* **16**, 1709 (2004)
- 5 K. Otsuka, *Appl. Opt.* **33**, 1111 (1994)
- 6 G. Giuliani, S. Bozzi-Pietra, S. Donati, *Meas. Sci. Technol.* **14**, 24 (2003)
- 7 E. Lacot, R. Day, F. Stoeckel, *Opt. Lett.* **24**, 744 (1999)
- 8 K. Otsuka, K. Abe, J.Y. Ko, T.S. Lim, *Opt. Lett.* **27**, 1339 (2002)
- 9 S. Donati, G. Giuliani, S. Merlo, *IEEE J. Quantum Electron.* **QE-31**, 113 (1985)
- 10 S. Donati, *Electro-Optical Instrumentation* (Prentice Hall, Hemel Hempstead, 2004)
- 11 S. Donati, *J. Appl. Phys.* **49**, 495 (1978)
- 12 P. Nerin, P. Puget, P. Besesty, G. Chartier, *Electron. Lett.* **33**, 491 (1997)
- 13 L. Keruevan, H. Gilles, S. Girard, M. Laroche, Y. Monfort, *Appl. Opt.* **28**, 4084 (2006)
- 14 N.D. Lai, M. Brunel, F. Bretenaker, B. Ferrand, L. Fulbert, *Opt. Lett.* **28**, 328 (2003)
- 15 M. Brunel, A. Amon, M. Vallet, *Opt. Lett.* **30**, 2418 (2005)
- 16 A. Le Floch, G. Stefan, C.R. Acad. Sci. Paris **277**, B265 (1973)
- 17 M. Sargent III, M.O. Scully, W.E. Lamb Jr., *Laser Physics* (Addison-Wesley, Reading, MA, 1974)
- 18 D.E. McCumber, *Phys. Rev.* **141**, 306 (1966)
- 19 R. Lang, K. Kobayashi, *IEEE J. Quantum Electron.* **QE-16**, 347 (1980)
- 20 E. Lacot, R. Day, F. Stoeckel, *Phys. Rev. A* **64**, 043815 (2001)
- 21 L. Morvan, N. Diep Lai, D. Dolfi, J.P. Huignard, M. Brunel, F. Bretenaker, A. Le Floch, *Appl. Opt.* **41**, 5702 (2002)
- 22 K. Otsuka, K. Abe, N. Sano, S. Sudo, J.-Y. Ko, *Appl. Opt.* **44**, 1709 (2005)